18TH WORLD CONFERENCE ON EARTHQUAKE ENGINEERING
WCEE2024
MILAN

MILAN, ITALY
30TH JUNE - 5TH JULY 2024
www.wcee2024.it

A NUMERICAL MODEL FOR THE MULTI-AXIAL RESPONSE OF HIGH DAMPING RUBBER BEARINGS

José A. Gallardo[1,2], Juan C. de la Llera[1,2], José I. Restrepo[3] & Michelle Chen[3]

[1] Department of Structural and Geotechnical Engineering, Pontificia Universidad Católica de Chile, Santiago, Chile, jogallardo@uc.cl

[2] Research Center for Integrated Disaster Risk Management (CIGIDEN), Santiago, Chile

[3] Department of Structural Engineering, University of California, San Diego, 9500 Gilman Dr., La Jolla, CA 92093, USA

Abstract: *The earthquake response of seismically isolated structures is largely controlled by the force-deformation constitutive behavior of the isolation devices. Thus, the modeling assumptions of this behavior in the isolators play a critical role in the performance assessment of these structures. Currently, High Damping Rubber Bearings (HDRBs) are widely used in practice, but their behavior is highly nonlinear and quite challenging to simulate numerically. With that objective in mind, this paper presents a new mathematical model to simulate the multi-axial behavior of HDRBs, including the numerical implementation of most of the phenomena present in such behavior. The proposed model considers a new stiffness degradation law, load-direction dependency, and axial-shear coupling. The latter is considered by the well-known two spring model, but includes an improvement based on experimental results. The proposed model fits reasonably well the experimental shear and axial response results of the isolators for different load patterns considered in the following validation tests: (i) bi-directional shear tests under rotated directions, aimed to prove the capacity of the model to simulate stiffness degradation with load-direction dependency; (ii) general bi-directional shear response, aimed to account for the coupling force effects between shear directions; (iii) isolator response histories; and (iv) extremely large deformations, aimed to prove that the model can simulate the response of the devices until the onset of failure. We conclude that this model, currently implemented in OpenSees, is sufficiently accurate and can effectively simulate the static and dynamic responses of buildings with HDRBs under multi-axial excitations. Moreover, the rather simple numerical implementation allows its direct use and adaptation into different available structural engineering software.*

1. Introduction

Over the las two decades, the performance-based earthquake engineering (PBEE) framework has attracted increasing attention. One of the key aspects of this approach is the explicit incorporation of the nonlinear behavior into the critical elements of the structure. Therefore, the availability of accurate force-deformation constitutive models for simulating the response of different materials and elements is essential. For the case of seismically isolated structures, technique that has gained popularity during a couple of decades, the seismic response is predominantly controlled by the force-deformation constitutive behavior of the isolation devices. Thus, the modelling assumption for the isolators determines the dynamic response of the complete building, and consequently, conditions its performance and capacity.

Currently, High Damping Rubber Bearings (HDRBs) are widely used in practice. These isolation devices, produced by vulcanizing interspersed layers of rubber and steel shims, are highly nonlinear and still present challenges for their numerical simulation. Some of the characteristic phenomena in their constitutive behavior are the bi-directional shear response; stiffness degradation with load-direction dependency, including scragging, or long-term degradation, and Mullins effect, or short-term degradation; strain-rate dependency; temporary hardening; coupling between axial and shear response, including axial stiffness softening due to increase of lateral displacement and shear stiffness variability due to axial load variation; and cavitation. Although the literature is rich in numerical models for simulating the behavior of HDRBs, most of them neglect important aspects of the multi-axial response of these devices, such as some of the previously mentioned phenomena or the coupling between different degrees of freedom. Furthermore, the typical approach for simulating the response of HDRBs is to connect two nodes using six springs (Kumar and Whittaker 2018), where each one represents the response in one of the six degrees of freedom: axial (1), shear (2), bending, (2) and torsion (1). The effect of those simplifications may be critical in seismic performance assessments, e.g., neglecting the stiffening at large deformations (Alhan et al. 2016).

Therefore, this manuscript presents a recently proposed numerical model for predicting the multi-axial behavior of HDRBs (Gallardo et al. 2023), which is sufficiently accurate and versatile for simulating the static and dynamic responses of seismically isolated structures. The model includes several of the most important phenomena present in this kind of devices, such as bi-directional shear coupling, stiffness degradation with load-direction dependency and axial-shear coupling. Additionally, an implementation of the model as a new element into OpenSees (Mckenna et al., 2000) is also provided.

2. Mathematical formulation

In this section, a brief description of the numerical model is presented, despite that the complete mathematical formulation can be found in Gallardo et al. (2024). The new element is based on the Two Spring Model (TSM) proposed by Koh and Kelly (1988), which explicitly incorporates the axial-shear coupling. Figures 1a and 1b summarize the mechanical behavior of the TSM in a 2D view.

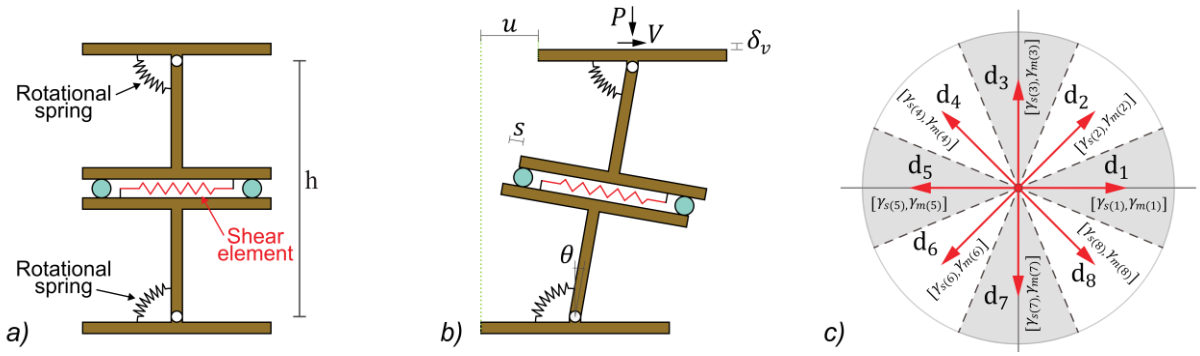

Figure 1. Sketch of the a) TSM undeformed and b) deformed configuration (adapted from Ryan et al. 2005), and c) the bi-directional shear element considering eight directions.

From Figure 1b, the geometric relations for the lateral and vertical deformations, simplified by considering small rotations, can be defined as

$$\delta_v = \boldsymbol{s\theta} + \frac{h\boldsymbol{\theta}^2}{2}, \tag{1}$$

$$\boldsymbol{u} = \boldsymbol{s} + h\boldsymbol{\theta}, \tag{2}$$

where h is the total height of the device, $\boldsymbol{u}$ is the lateral deformation, and $\boldsymbol{\theta}$ is the rotation of the rotational spring, and the equilibrium equations (forces and moments) are

$$\boldsymbol{V} = \boldsymbol{F}_s - P\boldsymbol{\theta}, \tag{3}$$

$$\boldsymbol{V}h - k_b\boldsymbol{\theta} + P(\boldsymbol{s} + h\boldsymbol{\theta}) = \boldsymbol{0}, \tag{4}$$

where $\boldsymbol{V}$ is the vector with bi-directional shear forces, $\boldsymbol{F}_s$ is the force of the bi-directional shear spring and k_b is the sum of stiffnesses of both rotational springs (the model was developed considering circular- or annular-shaped devices where the stiffness in both rotational directions has the same value).

The parameter δ_v represents the vertical deformation as a consequence of lateral deformation of the device. Thus, the total vertical deformation v is computed as

$$v = v_0 + \delta_v, \tag{5}$$

where v_0 is the vertical deformation in absence of lateral deformation. The additional deformation, generated due to the lateral deformation, can be considered as softening in the total vertical stiffness. Therefore, softening ratio can be computed as

$$\frac{K_v}{K_{v0}} = \frac{1}{1 + \frac{f_{as}|\boldsymbol{u}|}{\pi^2 R^*}}, \tag{6}$$

where K_v is the vertical stiffness in the deformed element, K_{v0} is the vertical stiffness of the bearing with zero lateral displacement, f_{as} is a parameter thar controls the softening ratio, and R^* is a factor that depends on the geometry of the devices. For the case of an annular-shaped bearing, it is defined as

$$R^* = \sqrt{1 + \left(\frac{D_i}{D_o}\right)^2}\ \frac{D_o}{4}, \tag{7}$$

where D_i and D_o are the inner and outer diameter, respectively. The relations R^* for other shapes can be found in Yang et al. (2017). Eq. 6 is derived from the TSM and considering the traditional theory for incompressible materials (the complete derivation can be found in Warn et al. 2007), which lead to a value of 3.0 for the factor f_{as}. However, experimental results (Chen et al. 2021) shows that this value could depend on the material and the stress state (Gallardo et al. 2024).

The response of the rotational springs is considered as linear-elastic, and can be easily replaced by any nonlinear model proposed in the literature (e.g., Nagarajaiah and Ferrel 1999, Vemuru et al., 2014).

The rheological model for the bi-directional shear spring considers a hyperelastic and dissipative components working in parallel. Thus, the shear force $\boldsymbol{F}_s$is defined as

$$\boldsymbol{F}_s = \boldsymbol{F}_h + \boldsymbol{F}_d, \tag{8}$$

where $\boldsymbol{F}_h$ and $\boldsymbol{F}_d$ are forces of the hyperelastic and dissipative component, respectively.

The force of the hyperelastic component is computed as

$$\boldsymbol{F}_h = [a_{10}k_{s1}k_m|\boldsymbol{\gamma}| + a_{20}k_{s2}|\boldsymbol{\gamma}|^3 + a_{30}k_{s3}|\boldsymbol{\gamma}|^5]\overline{\boldsymbol{\gamma}}, \tag{9}$$

where a_{10}, a_{20}, and a_{30} are constants that depend on the material and cross section area of the rubber layers; k_{s1}, k_{s2}, and k_{s3} are the scragging factors (long-term degradation); k_m is the Mullins effect factor (short-term degradation); $|\boldsymbol{\gamma}|$ and $\overline{\boldsymbol{\gamma}}$ are the Euclidean norm and unit vector of $\boldsymbol{\gamma}$, being $\boldsymbol{\gamma}$ the shear strain ($\boldsymbol{s}/H_r$, where H_r is the total height of rubber in the device). The stiffness degradation parameters are computed as follows

$$k_{s1} = \exp(-C_1{\gamma_s}^{P_1}), \tag{10}$$

$$k_{s2} = k_{s1}\exp(-C_2{\gamma_s}^{P_2}), \tag{11}$$

$$k_{s3} = k_{s1}\exp(-C_3{\gamma_s}^{P_3}), \tag{12}$$

$$k_m = \exp(-C_m{\gamma_m}^{P_m}), \tag{13}$$

where γ_s and γ_m are the considered strain for scragging and Mullins effect, respectively, this factor varies depending on the deformation direction (see Figure 1c); and the parameters C_i and P_i are material properties. The load direction dependency is incorporated using a modified version of the material directions theory. The complete spectrum of strain shear directions is divided into a finite number of spaces, each one characterized by the unit vector of the direction and by its own considered strains for scragging (γ_s) and Mullins effect (γ_m). It is worth nothing that there is coupling between the evolution of the considered strains of different directions,

which generates the load direction dependency. The complete degradation model is presented in Gallardo et al. (2024).

The dissipative component is defined using the Bouc-Wen model with hardening (Karavasilis et al. 2012), whose force is computed as

$$\boldsymbol{F_d} = f_y \boldsymbol{z}, \tag{14}$$

where f_y is the yield force of the bearing, and $\boldsymbol{z}$ is a dimensionless hysteretic parameter. The rate equation of the latter is defined as

$$\dot{\boldsymbol{z}} = \left(k/f_y\right)\left[\,\dot{\boldsymbol{\gamma}} - \boldsymbol{z}R\right], \tag{15}$$

where k is the elastic stiffness, $\dot{\boldsymbol{\gamma}}$ is the shear strain rate, and R is a factor defined as

$$R = \left[(\beta-\varphi)\left(|\dot{\gamma}_x z_x| + |\dot{\gamma}_y z_y|\right) + (\alpha-\varphi)\left(\dot{\gamma}_x z_x + \dot{\gamma}_y z_y\right)\right]\left({z_x}^2 + {z_y}^2\right)^{\frac{\eta-2}{2}}, \tag{16}$$

where β and α are parameters that control the shape of the cycle and satisfy the relation $\beta + \alpha = 1$; η controls the sharpness of the smooth transition from the elastic to the inelastic zone; and the parameter φ quantifies the hardening. The definition of the parameter φ, and more details of the formulation can be found in Gallardo et al. (2024).

3. Results

The results of the model under four different load patters are presented in this section. It includes: (i) bi-directional shear tests under rotated directions; (ii) general bi-directional shear response; (iii) response history analysis; and (iv) test under extremely large deformations.

First, bi-directional shear tests of cylindrical disks are performed, the experimental campaign carried out by Ragni et al. (2018) was considered as reference. Thus, just the model for the bi-directional shear spring is evaluated. The deformation history of the specimens consists of two deformation sequences: first, six cycles in the reference direction ($\theta = 0°$), the test stops, the specimen is rotated ($\theta = 0°, 90°, 180°$), and then other six deformation cycles. This procedure is performed for five strain amplitudes: 0.25, 0.50, 1.0, 1.50, and 2.50. The diagram of the test in presented in Figure 2a.

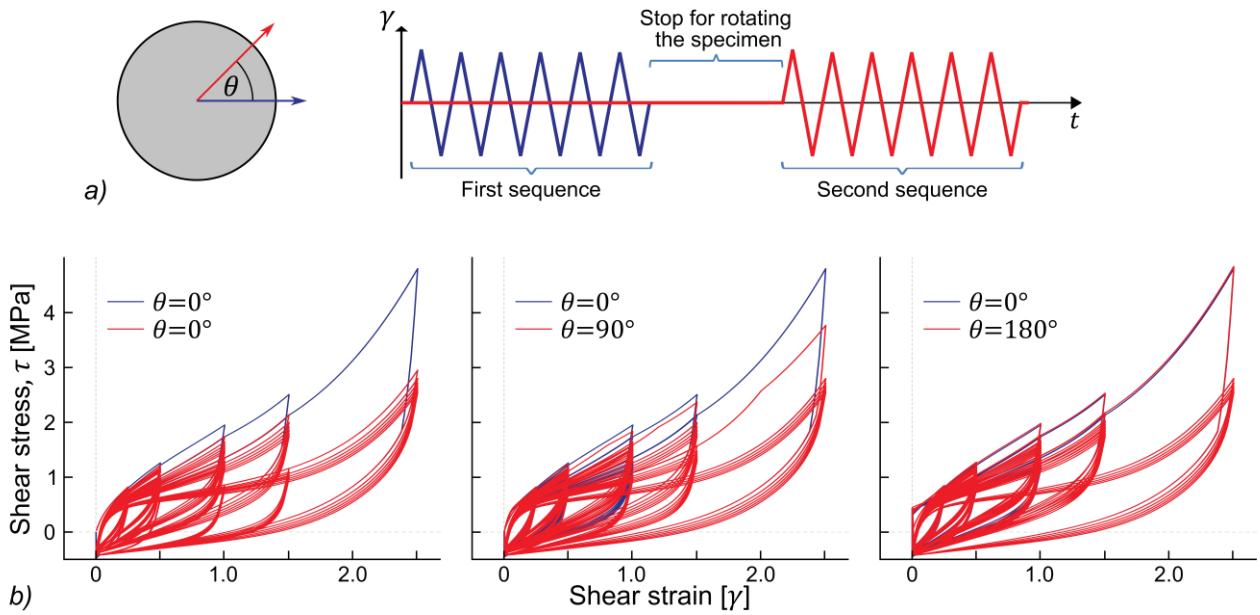

Figure 2. a) Sketch of the load pattern and b) numerical response of the double shear tests on rotated directions.

All results presented in Figure 2 are consistent with the experimental results presented by Ragni et al. (2018). When the rotation angle is zero (Figure 2b), the parameter that controls Mullins effect reboots, which accounts for the recovery of the short-term degradation due to the stop for rotate the specimen. An increase in the rotation angle generates an increase of the force in the second sequence (red line), it is because of the load direction dependency (anisotropic degradation). The effect of the first sequence (degradation) decrease as the rotation angle increases, such as with a rotation of 180° (maximum), there is no coupling effect (the called unilateral effect presented by Gallardo et al. 2023). When the rotation angle equals 90° (Figure 2b), some degradation can be noticed during the second sequence as a consequence of the first sequence. Thus, the model can simulate the load direction dependency of the rubber material under shear deformations.

Secondly, the bi-directional shear response of the HDRB tested by Chen et al. (2021) was simulated. The load pattern applied to the device consisted of a constant compressive force and a deformation history with an elliptical orbit in the horizontal plane (see Fig. 3a). Given that the device was previously tested under several load patters, the response does not present long-term degradation.

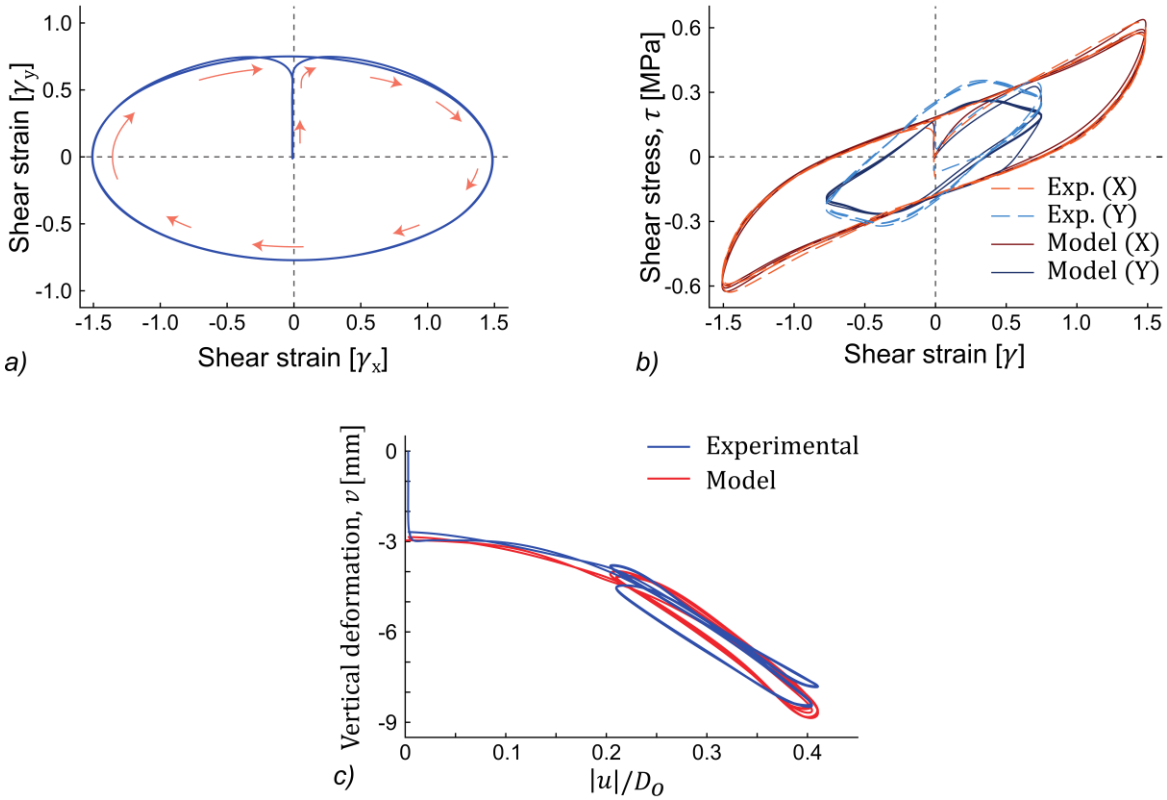

Figure 3. Comparison between the bi-directional experimental test and the numerical results: (a) shear deformation pattern; (b) shear stress versus deformation; and (c) vertical versus lateral deformation normalized by the outer diameter.

The shear deformation response (Fig. 2b) of the numerical model in the longitudinal direction fits the experimental result well while it differs from the experimental response in the transverse direction, which shows a hump protruding the response in the longitudinal direction. This stiffer response is a consequence of anisotropic degradation, while the negative slope after the peak is the effect of bi-directional coupling. The numerical response fits the experimental result reasonably well. The hump due to large anisotropy degradation is not reproduced exactly in magnitude but is reproduced in shape. Figure 3c shows the vertical deformation versus the normalized lateral deformation normalized by the outer diameter of the device. The model can effectively simulate the vertical softening due to the lateral deformation of the device.

Third, the response history analysis of the device tested by Chen et al. (2021) was simulated. The test protocol consisted in a compression load to the device (which slightly varies during the test), and then the shear displacement history is applied (it was a uni-directional test).

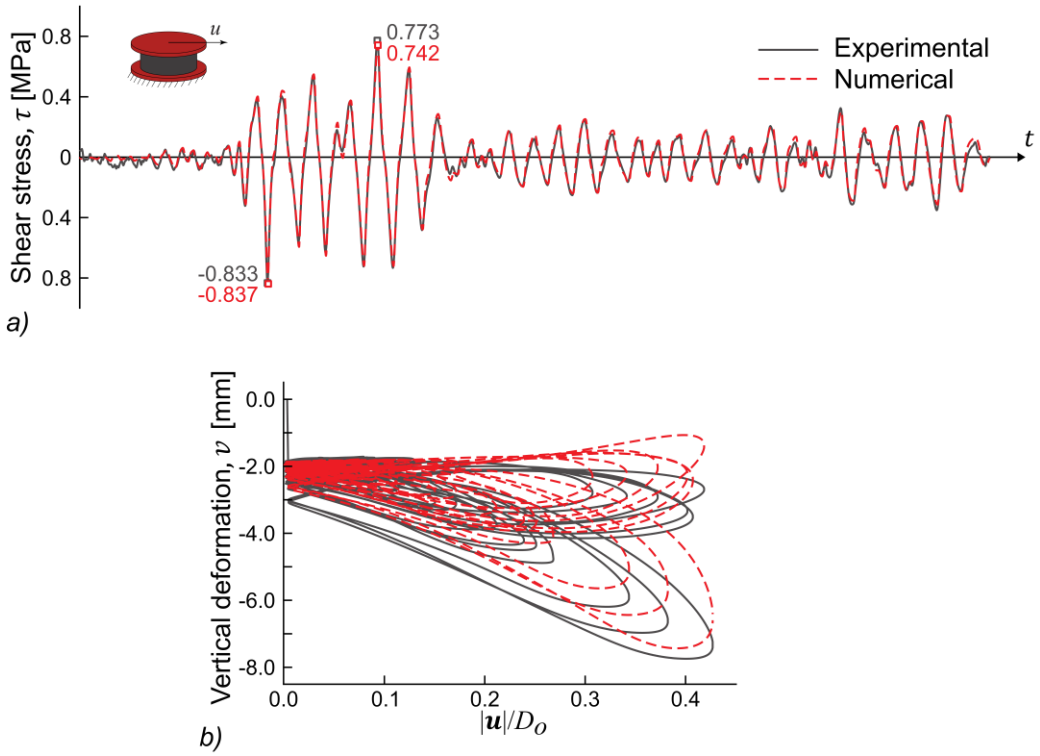

Figure 4. Comparison of the dynamic responses between the experimental test and numerical results: (a) response-history of shear stress, and (b) vertical versus lateral deformation normalized by the outer diameter.

Figure 4 shows the shear stress history and vertical deformation versus lateral deformation normalized by the outer diameter of the numerical model. It is worth nothing that the parameter calibration was performed using experimental results of cyclic shear tests and not the results of the response history analysis. The presented model simulates very well the experimental result of the device under the displacement history. The differences on the positive and negative peaks are of 4.2 and 0.5%, respectively. Larger differences can be noticed at the beginning of the test, where the response is mostly linear, it is a consequence of different initial stiffness values. Thus, although the model is strain-rate independent, it can accurately simulate the dynamic behavior of HDRBs.

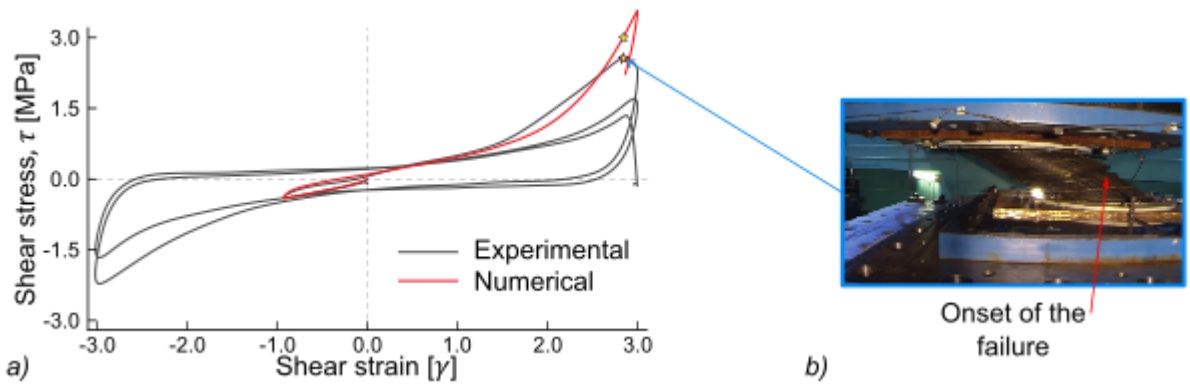

Figure 5. a) Comparison of the experimental test and numerical response for extremely large deformations and b) picture of the specimen at the onset of the failure.

Fourth, the response of a HDRB under extremely large deformation is simulated. With this goal in mind, the failure test presented by Chen et al. (2021) was simulated. The load pattern consisted of a compression load applied to the device and a cyclic shear deformation history. During the experimental test, the failure was

triggered during the first cycle at $\gamma \approx 2.70$, and since the numerical model does not consider the failure mechanism, the comparison is valid only up to that strain value.

Figure 5 shows the comparison of the numerical and experimental results. The numerical model simulates reasonably well the response of the device until de onset of the failure, and it overestimates the shear force for deformations beyond this point. The parameters of the model were calibrated using the experimental results the first cyclic deformation history at which the device was subjected to consider the behavior of the virgin material. It is also important to highlight that the numerical model considers that the material has not been deformed beyond $\gamma = 1.50$ previously.

4. Numerical implementation

The model presented herein was implemented in OpenSees (Mckenna et al., 2000), and is openly available through the repository https://github.com/JAGallardo1992/HDRB_model. Meanwhile the pseudo-code for this implementation can be found in Gallardo et al. (2024).

5. Conclusions

This manuscript presents a new element to simulate the multi-axial response of High Damping Rubber Bearings (HDRBs). The element considers the Two Spring Model (TSM) for including the axial-shear coupling but introduce a modification for the axial softening due to lateral deformation. The rotational springs are considered as linear-elastic, but can easily be replaced by a different model. The bi-directional shear spring simulates the response considering two elements working in parallel: a hyperelastic and dissipative components. The former includes stiffening at large deformations and stiffness degradation with load direction dependency (anisotropic degradation), which is formulated using a modified version of the material directions theory. The dissipative component includes temporary hardening. The presented model simulates well the response of the devices under several load patterns, proving that:

- It can reproduce the load direction dependency of the elastomeric material reasonably well.
- The softening of the axial stiffness due to lateral deformation can be captured, and the f_{as} parameter regulates the softening rate.
- It can simulate the dynamic response of the devices reasonably well, with error lower than 5% for the peak values.
- It can reproduce the response of the devices until the onset of the failure, although experimental results of the device under smaller deformations are used for the parameter calibration.

The presented model has been implemented into the OpenSees software and is openly available, which facilitates their use in the performance assessment of structures.

6. Acknowledgments

This research has been sponsored by ANID/doctorate scholarship/ 21201370, Re-search Center for Integrated Disaster Risk Management (CIGIDEN), ANID/ FONDAP/ 15110017; and FONDECYT project, Multiscale earthquake risk mitigation of healthcare networks using seismic isolation, ANID/ FONDECYT/ 1220292.

7. References

Alhan C., Gazi H., Kurtuluş H. (2016). Significance of stiffening of high damping rubber bearings on the response of base-isolated buildings under near-fault earthquakes. *Mechanical Systems and Signal Processing*, 79, 297-313.

Chen M.C., Benzoni G., Restrepo J.I. (2021). Response of a high damping rubber bearing to multiaxial excitation. *Journal of Testing and Evaluation*, 49(2), 1153-1172.

Gallardo J.A., de la Llera J.C., Restrepo J.I., Chen, M. (2023). A numerical model for non-linear shear behavior of high damping rubber bearings. *Engineering Structures*, 289, 116234.

Gallardo J.A., de la Llera J.C., Restrepo J.I., Chen, M. (2024). Modeling the multi-axial behavior of High Damping Rubber Bearings (HDRBs). *Under review*.

Karavasilis T.L., Kerawala S., Hale E. (2012). Hysteretic model for steel energy dissipation devices and evaluation of a minimal-damage seismic design approach for steel buildings. *Journal of Constructional Steel Research*, 70, 358-367.

Koh C.G., Kelly J.M. (1988). A simple mechanical model for elastomeric bearings used in base isolation. *International journal of mechanical sciences*, 30(12), 933-943.

Kumar M., Whittaker A.S. (2018). Cross-platform implementation, verification and validation of advanced mathematical models of elastomeric seismic isolation bearings. *Engineering Structures*, 175, 926-943.

McKenna F., Fenves G.L. and Scott, M.H. (2000). Open system for earthquake engineering simulation. *University of California, Berkeley, CA*.

Nagarajaiah S., Ferrell K. (1999). Stability of elastomeric seismic isolation bearings. *Journal of Structural Engineering*, 125(9), 946-954.

Ragni L., Tubaldi E., Dall'Asta A., Ahmadi H., Muhr, A. (2018). Biaxial shear behaviour of HDNR with Mullins effect and deformation-induced anisotropy. *Engineering Structures*, 154, 78-92.

Ryan K.L., Kelly J.M., Chopra, A.K. (2005). Nonlinear model for lead–rubber bearings including axial-load effects. *Journal of engineering mechanics*, 131(12), 1270-1278.

Vemuru V.S.M., Nagarajaiah S., Masroor A., Mosqueda G. (2014). Dynamic lateral stability of elastomeric seismic isolation bearings. *Journal of structural engineering*, 140(8), A4014014.

Warn G.P., Whittaker A.S., Constantinou M.C. (2007). Vertical stiffness of elastomeric and lead–rubber seismic isolation bearings. *Journal of structural engineering*, 133(9), 1227-1236.

Yang W., Sun X., Wang M., Liu P. (2017). Vertical stiffness degradation of laminated rubber bearings under lateral deformation. *Construction and Building Materials*, 152, 310-318.